Fire ants self-assemble into waterproof rafts to survive floods

Nathan J. Mlot[a], Craig A. Tovey[b], and David L. Hu[a,c,1]

[a]Schools of Mechanical Engineering, [b]Industrial and Systems Engineering, and [c]Biology, Georgia Institute of Technology, Atlanta, GA 30318

Edited by Charles S. Peskin, New York University, New York, NY, and approved March 31, 2011 (received for review November 8, 2010)

Why does a single fire ant *Solenopsis invicta* struggle in water, whereas a group can float effortlessly for days? We use time-lapse photography to investigate how fire ants *S. invicta* link their bodies together to build waterproof rafts. Although water repellency in nature has been previously viewed as a static material property of plant leaves and insect cuticles, we here demonstrate a self-assembled hydrophobic surface. We find that ants can considerably enhance their water repellency by linking their bodies together, a process analogous to the weaving of a waterproof fabric. We present a model for the rate of raft construction based on observations of ant trajectories atop the raft. Central to the construction process is the trapping of ants at the raft edge by their neighbors, suggesting that some "cooperative" behaviors may rely upon coercion.

cooperative animal behavior | surface tension | adhesive | emergent | differential equation

The cooperative behavior of flocks, schools, and swarms has received much attention by biologists (1, 2), mathematicians (3, 4), and roboticists (5, 6). Ants are particularly well known for their ability to work together to complete complex tasks such as foraging, nest construction, and food cultivation (7). In this study, we consider the fire ant *Solenopsis invicta*, originally from the rainforests of Brazil (8). Due to the regular flooding of its habitat, this ant has evolved striking behaviors to keep its colonies together. Among these include the construction of self-assemblages, such as ladders, chains, walls, and rafts, composed exclusively of individual ants linked together tarsus-by-tarsus (9–11). The raft is one of the longest-lasting structures, allowing ants to sail upon it for months as they migrate and colonize new lands (12).

A raft is defined as a flat vessel for flotation or transport on water. Usually, it is characterized by the lack of a hull and floats simply by the buoyancy of its materials rather than by watertight integrity. By Archimedes' Law, the buoyancy force of a raft is given by $(\rho - \rho_w)Vg$ where g is gravity, V is the displaced volume of the fluid, and ρ and ρ_w are the densities of the raft materials and water, respectively. Using low-density materials is thus a necessity, as was known in 5,000 B.C. when the first rafts were built by humans using logs and twine (13). In the natural world, aquatic plants raft by virtue of the air stored in underwater stolons. Animals generally cannot trap air pockets in this manner and so instead raft by stowing away upon mats of floating vegetation (14).

Individual ants may float if the water surface is free of surfactants. Although denser than water, they rely upon surface tension forces in the manner of water-walking insects and certain biomimetic robots (15–17). However, surface tension is generally too weak to support objects that have the density of water and a size much larger than the capillary length $\ell_c = \sqrt{\sigma_w/(\rho_w g)} \approx 2.3$ mm, where σ_w is the surface tension of water. Consequently, it is not immediately obvious how colonies of thousands of ants can float so easily.

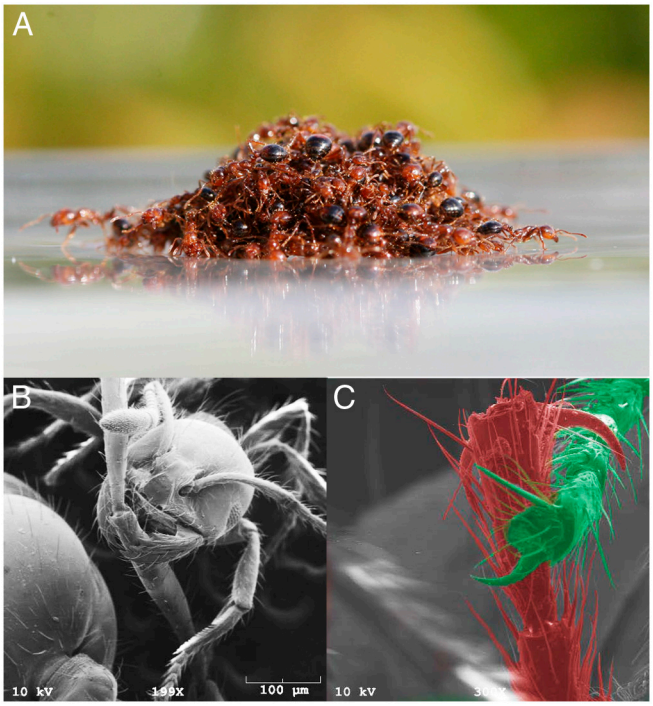

Fig. 1. (*A*) A raft of 500 fire ants, composed of a partially wetted layer of ants on the bottom and dry ants on top. (*B* and *C*) Scanning electron micrographs of links between ants in the raft, consisting of mandible–tarsus and tarsus–tarsus attachments. Note that the mandibular grip requires particular care to minimize pain to the recipient of the bite.

Results

We conducted a series of laboratory experiments to determine how ants respond to floods, from which we observed ants constructing rafts when placed into water. A small ant raft (500 ants) in water free of surfactants is shown in Fig. 1*A* and Movie S1; rafts of 3,000 and 8,000 ants are shown in Movies S2, S3, S4, and S5. Fire ant colonies were collected from local roadsides in Atlanta, cared for, and filmed in our laboratory (see *Methods* and *SI Text* for details).

Fire ants in a colony vary in size, with heights of 0.5–2.5 mm, lengths of 1–4.5 mm, and masses of 0.5–5 mg (18). Their average mass, 1.3 ± 0.8 mg ($N = 16$), was used to estimate the number of ants in a raft. We characterized ant rafts by a planar ant packing of $\gamma = 34 \pm 2$ ($N = 4$) ants per cm^2, found by counting ants in four rafts of fixed size. This packing corresponds to a distance

Author contributions: N.M., C.T., and D.H. and designed research, performed research, analyzed data, and wrote the paper.

The authors declare no conflict of interest.

This article is a PNAS Direct Submission.

[1]To whom correspondence should be addressed. E-mail: hu@me.gatech.edu.

This article contains supporting information online at www.pnas.org/lookup/suppl/doi:10.1073/pnas.1016658108/-/DCSupplemental.

between ant centers-of-mass of $\delta = 1/\sqrt{\gamma} = 0.17 \pm 0.02$ cm. The average ant speed while walking on the raft is $u \approx 0.39 \pm 0.18$ cm/s ($N = 8$), measured by observing ants atop the raft.

Cohesive Strength. We froze ant rafts in liquid nitrogen to visualize how ants are linked together within the raft. We find that ants grip each other by using a combination of mandibles, tarsal claws, and adhesive pads located on the ends of their tarsi (Fig. 1 *B* and *C*). We observed that frozen ant rafts are brittle, disintegrating upon handling, and so infer that the strength of ant gripping depends on the squeezing force applied by the ant's grip. By harnessing two live ants with an elastic band, we found that the maximum tensile force between them is $F = 620 \pm 100$ dyn ($N = 11$), or more than 400 times body weight. This force is significantly weaker than ant attachment forces to other complex surfaces. One example is the velcro-like attachment (5,700 times body weight) between ant claws and the fuzzy loops on certain plant leaves (19). Conversely, the gripping force is twice as strong as the ant adhesion to smooth surfaces such as glass (370 ± 90 dyn, $N = 10$) or plastic (1–150 times body weight) (20, 21). On such surfaces, ants extrude fluid drops with their feet, adhering using the associated capillary and viscous forces (18, 22, 23).

When many ants are placed in a beaker, they readily clump, forming a porous viscoelastic material. The material can be easily broken apart by hand, without injuring any of the ants. This low cohesion is consistent with rough estimations of the ant matrix tensile strength, $\sigma_f \approx F/\delta^2 \approx 2 \times 10^4$ dyn/cm^2 = 2,000 Pa, which is several orders of magnitude less than the strength (10^6 Pa) of connective stolons of floating plants (24). However, the strength is sufficient to hold an ant raft together on the water surface. We note that the cohesion of the ants is highly dependent on the water surface being clean. Traces of surfactant cause ants to release their grip upon each other, causing the raft to fall apart and sink (Fig. S1). It is thus possible that ant-to-ant cohesion on the water surface may be aided by capillary forces, which have been shown to help other insects aggregate on the water surface (25).

Water Repellency and Buoyancy. In order to prevent dehydration or bacterial growth, many natural surfaces are water repellent. On plant leaves (26) and insect cuticle (27, 28), water drops bead up, demonstrating high contact angles θ_e with the solid. As shown in Fig. 2*A*, an ant's cuticle is mildly hydrophobic, with a contact angle θ_e of $102 \pm 4°$ ($N = 10$), a value consistent with measurements on other terrestrial insects (28). An advantage of being hydrophobic is the ability of ants and semiaquatic insects to trap a plastron layer of air around their bodies, without which they would sink. We verified the necessity of the plastron by measuring the volume displacement of ant rafts. We find that clean water permits plastron retention, whereas soapy water prevents it. The average material density of ants was measured by $\rho = m/V$, where m is their mass and V the volume of water they displaced when submerged. We found that their average density without plastrons was 1.1 ± 0.3 g/mL ($N = 3$), which is greater than the density of water. Thus, ants in soapy water will struggle to swim and eventually sink. In clean water, however, ants are clearly able to trap plastrons, as shown by the bubbles attached to submerged ants (Fig. 2*D*). These bubbles are enlarged in submerged ant rafts, as shown by the large air pockets in Fig. 2*E*. These trapped air pockets decrease their mean density by 75% to $\rho = 0.2 \pm 0.04$ g/mL ($N = 4$). The presence of the plastron also explains why ants in rafts rarely drown: Their plastron enables them to breathe even when they are at the bottom of the raft.

To understand why water does not penetrate a raft, we investigated its water repellency. We deposited drops on ant rafts and observed that the contact angles of ant rafts were $133 \pm 12°$ ($N = 6$), which is 30% higher than that of individual ants

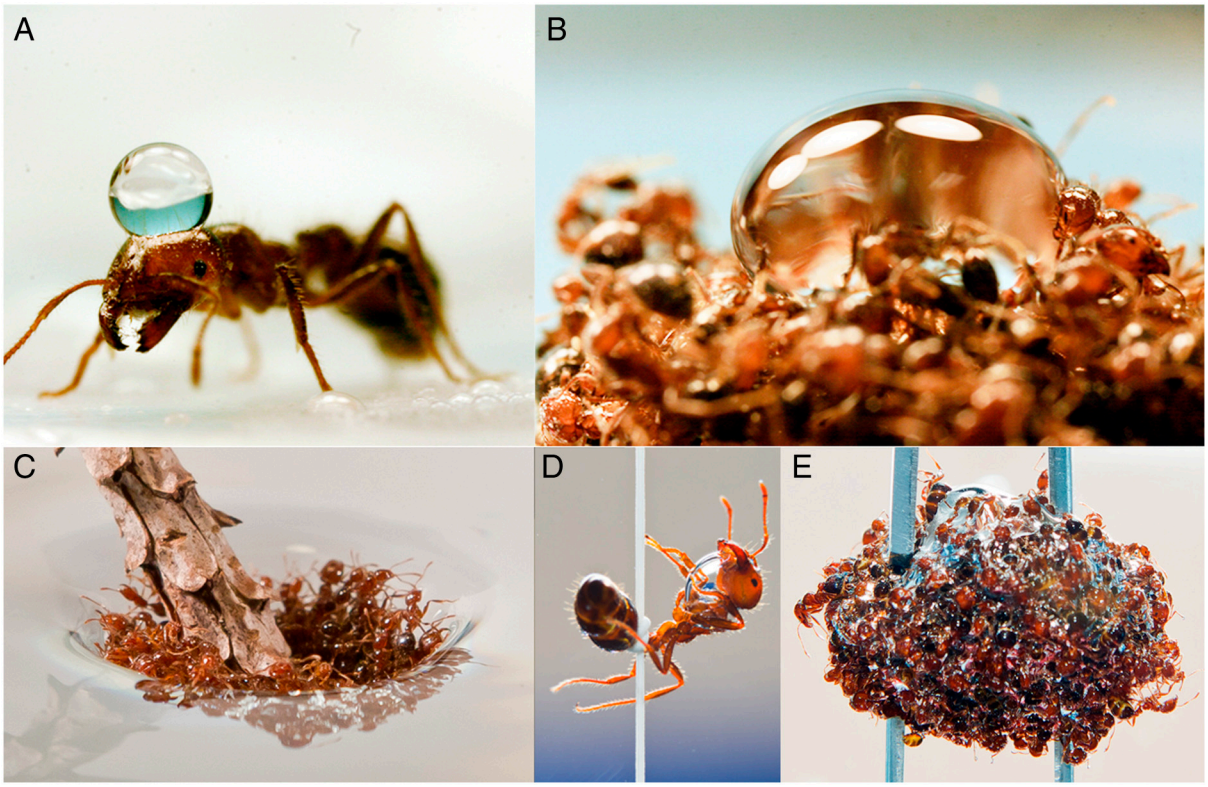

Fig. 2. Water repellency of the ant rafts. (*A*) An individual ant's exoskeleton is moderately hydrophobic, as shown by the contact angle of the water drop. (*B*) Enhanced water repellency of a raft of ants, as shown by the increased contact angle of the water drop. (*C*) Buoyancy and elasticity of the ant raft, as shown by attempted submersion by a twig. (*D*) The plastron air bubble of an ant in soap-free water. The bubble makes the ant buoyant, necessitating the use of a thread to hold it underwater. (*E*) An air pocket trapped in a submerged ant raft. The shimmery layer around the ants is the air–water interface.

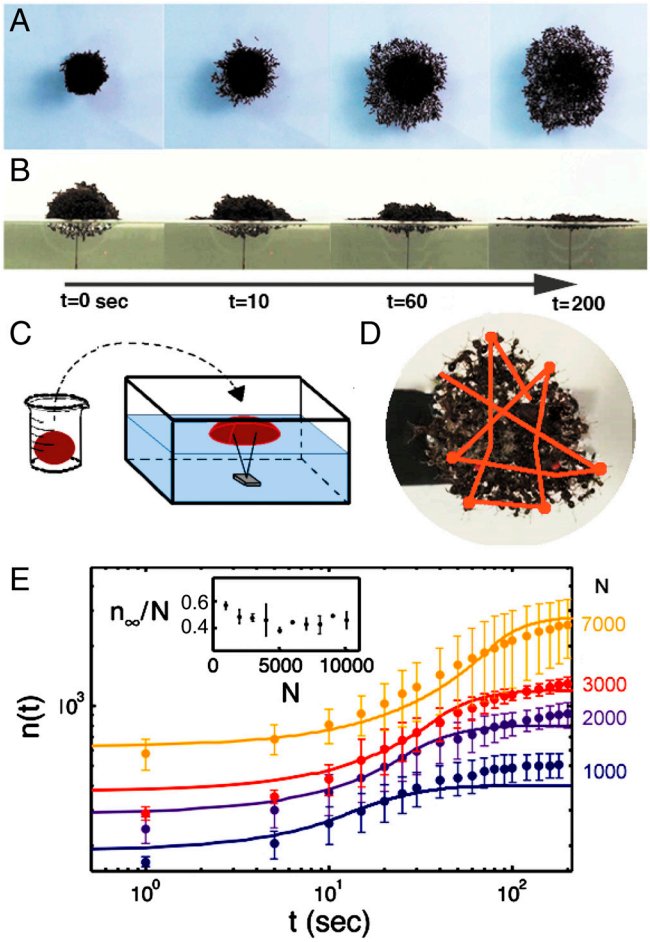

Fig. 3. Dynamics of ant-raft construction. (*A* and *B*) Top and side views of growth of a 3,000-ant raft. (*C*) Schematic of experimental setup. Ants are rolled into balls in a beaker and then placed onto a pronged stabilizer in a partially filled aquarium. (*D*) The trajectory of a single ant on the raft, tracked over a duration of 40 s. (*E*) The relation between time t and the number of ants on the bottom of the raft $n(t)$. Data are shown for four raft sizes, characterized by the number of ants in the raft N. Solid lines are given by the predictions of our theoretical model. (*Inset*) The relation between the number of ants in the raft N and the proportion of ants on the bottom at equilibrium n_∞/N.

(Fig. 2*B*). This water repellency is consistent with predictions using the Cassie–Baxter Law of wetting (28–30). This law states that the contact angle θ^* of a textured solid is given by the relation $\cos(\theta^*) = \phi(\cos\theta_e + 1) - 1$, where ϕ is the area fraction of the ant–water contact. Using the ant area fraction, $\phi = (\rho/\rho_w)^{2/3} = 0.35$, yields that $\theta^* = 136°$, which corresponds well with our observations. This enhanced water repellency prevents the raft from sinking when submerged (Fig. 2*C*) and aids in waterproofing during rainstorms. Although natural water repellency has been previously viewed as a static property of a surface (29), the ant raft represents a clear example of a surface rendered water repellent by cooperative behavior.

In response to mechanical perturbations or submergence (Fig. 2*D*), the ants contract their muscles in unison, squeezing the raft into a tight mass. Consequently, the raft suffers a slight loss of buoyancy due to the increased raft density, $\rho_{\max} = 0.27 \pm 0.01$ g/cm^3 ($N = 3$). A benefit of this behavior is the decrease in ant separation distance, which rigidifies the raft. Moreover, the tighter weave increases the submergence depth at which fluid imbibition occurs (28). A rough estimate of this depth, without taking into account the ants' legs, yields $z \sim 2\sigma/(\delta\rho_w g) \sim 1$ cm; in our experiments, we observed some air bubbles escaping at 3–10 cm and others remaining trapped at depths over 20 cm.

Table 1. Fluid properties of ants compared to water

	Density, g/mL	Dynamic viscosity, cP	Surface tension, dyn/cm
Water	1.0	0.89	72
Ant rafts	≈0.2	~10^6	~10^3

Construction Rate. We observed raft construction using spheres of ants, each containing $N = 1{,}000$–$7{,}000$ ants (Fig. 3*C*). Not surprisingly, ant spheres that are placed on solid surfaces quickly disintegrate as the ants flee in all directions. However, when placed on the water surface, ant spheres redistribute and reconnect themselves into a raft, as shown in the video sequence in Fig. 3 *A* and *B*. The raft reaches a stable equilibrium within several minutes. At equilibrium, the rafts are pancake shaped, whereby a dry portion of the colony stands atop a monolayer of stationary ants. The spreading of the raft resembles that of a drop of fluid, so we first consider modeling ants as a continuum.

Ants as a Fluid. Spreading drops have been studied in the context of water, blood, lava, and shampoo (31–33). By crudely estimating the continuum properties of ants, we may model the raft as a fluid composed of ant "molecules." Table 1 gives order-of-magnitude estimates for the density, viscosity, and surface tension of ants compared to water. The surface tension of ants, $\sigma = F/\delta$, was estimated using the characteristic ant force F and spacing δ. Ant viscosity was inferred from the very slow settling speed (10^{-2} cm/s) of a metal sphere in a beaker of ants (see *Methods*). Compared to water, ant rafts have one-fifth the density, but 10 times the surface tension and 10^6 times the viscosity. Their surface tension is 5 times higher than that of mercury (487 dyn/cm); and their viscosity is similar to that of high-viscosity silicone oil [10^6 cP (1 P = 0.1 Pa · s)]. The capillary length for ants is $L_a = 3$ cm, which is 10 times larger than that for water.

In our experiments, a sphere of $N = 3{,}000$ ants (with a volume Ω of 15 mL), spreads from $R = 1.5$ to 3.6 cm in 150 s. Given that ants are significantly more viscous than water, the physical picture of an ant raft is that of a viscous lens (a large pancake-shaped drop) floating on an immiscible nonviscous liquid. The associated physics is well understood and closed-form solutions have been derived by previous investigators (29, 33) for the final drop radius R as a function of time. Drops smaller than L_a spread at timescales of $t \sim (\pi/16)R^4/(\Omega\sigma/\mu)$; larger drops spread at timescales of $t \sim (1/2)R^2\mu/(\tilde{\rho}g\Omega)$, where ρ, μ, and σ are the density, viscosity, and surface tension of ants given in Table 1; Ω is the droplet volume; and $\tilde{\rho} = \rho(1 - \rho/\rho_w) = 0.25$ is the ant material density corrected for the Archimedes' pressure. Using these relations, we predict a spreading time of 10^3 s, which is nearly an order of magnitude greater than in our experiments.

In the lubrication limit of a spreading drop, flow is two-dimensional and radial: Fluid particles tend to follow the ones in front of them. Such simple flows have arisen in previous studies of ants —for example, in the raids of army ants, where they travel in straight lines, and in "circular ant mills," where ants travel in circles endlessly (7). Do rafting ants travel in such simple patterns? Tracking the trajectories of ants on rafts of various sizes, we find that they move using a stereotyped sequence of behaviors (as shown in Fig. 3*D*), including walking in straight lines, ricocheting off the edges of the raft, and walking again until finally adhering to an edge. The probability p that an ant will bounce off the raft edge, rather than sticking and adding to the edge, is $p = 0.64 \pm 0.04$ ($N = 5$). As shown in the *SI Text*, the expected travel distance on a unit disk during this sequence of randomly directed walks is $\alpha = \frac{8}{3\pi} + \frac{4}{\pi}\left(\frac{p}{1-p}\right) \approx 3.1$. The discrepancy between α and unity indicates a potential problem in modeling ants as fluids. One view of a spreading fluid drop is that of an ideal

APPLIED MATHEMATICS

cooperative organism in that all particles travel radially. In comparison, ant motion is not radial, but in fact so random that they must travel 3.1 times the drop radius to reach the edge of the raft.

Another potential problem in modeling ants as fluids is that such models suggest that ant rafts should spread according to simple power laws with respect to time. Fig. 3*E* shows the time course of the number of ants on the raft bottom n, with colors denoting the raft size, $N = 1{,}000$–$7{,}000$ ants ($N = 21$). The trends, plotted in log–log, are sigmoid rather than linear, indicating that a power law fails to account for ant-raft spreading. One last difference in the two systems is that ants are a source of kinetic energy, in contrast to a drop of fluid, in which gravitational energy is dissipated by viscosity. Given these discrepancies, we turn to a discrete model of ants, modeled as self-propelled independent agents.

Straight-Path Model. An important input parameter into our model is the raft thickness at equilibrium. Clearly, the ant raft has some topology as shown in Fig. 3*B*. We can estimate the spatially averaged thickness using n_∞, the number of ants on the bottom of the raft at time t_∞: The thickness is then $h = N/n_\infty \approx 2.5 \pm 0.4$ ($N = 30$) layers of ants. Physically, h corresponds to 8 mm, a quantity that appears to be conserved for all rafts. Fig. 3*E*, *Inset*, shows that the n_∞ is approximately $40 \pm 10\%$ the total number of ants, N. Thus, ant rafts appear to exhibit some level of fairness in that no more than half the colony is on the bottom of the raft. The selection of raft thickness is beyond the scope of this study; presumably, it results from a competition between raft strength and the ants' aversion to be on the bottom of the raft.

In our model, we assume that only the top layer of ants can move and the remaining layers of ants are jammed. In our model, we will thus distinguish two stages in the raft construction: short times for which $n(t) \leq N/(h+1)$, when a full top layer of ants may move, and long times, for which $n(t) > N/(h+1)$, when there is only a partial layer of $N - hn(t)$ ants that can move. Keeping track of these regimes is important because the number of ants on top strongly influences the deposition rate of ants at the edge.

If the ants have a uniform packing of γ (ants per square centimeter), the area of the raft can be written as a corresponding number of ants using $\pi r^2 = n(t)/\gamma$. The radius of the raft in centimeters is $r = \sqrt{n(t)/\gamma\pi}$. If there are $n(t)$ ants in the moving layer, on average $n(t)u/\alpha r$ ants attach to the boundary per second. Considering that the ants distribute themselves to form a new exterior boundary h ants thick, the rate of new ants on the bottom equals $\beta\sqrt{n(t)}$ numbers of ants per second, where $\beta = \frac{u\sqrt{\gamma\pi}}{\alpha h} \approx 0.52\ \mathrm{s}^{-1}$. Conversely, if there are $N - hn(t)$ ants in the moving layer, then $\beta(N - hn(t))/\sqrt{n(t)}$ add to the bottom per second. Thus, the rate of change in the number of ants $n(t)$ on the bottom layer at time t evolves according to

$$\frac{dn}{dt} = \begin{cases} \beta\sqrt{n(t)} & \text{if } n(t) \leq N/(h+1) \\ \beta(N - hn(t))/\sqrt{n(t)} & \text{if } n(t) > N/(h+1). \end{cases} \quad [1]$$

The initial values for the differential Eq. **1**, $n_0 \approx 2.6N^{0.62}$ were estimated using the number of ants in the cross-section of a sphere of N ants. Integrating Eq. **1**, we obtain the solution

$$\begin{aligned} n(t) &= \left(\tfrac{1}{2}\beta t + \sqrt{n_0}\right)^2 && \text{if } t \leq t^* \\ t - t^* &= -\tfrac{2}{\beta h}\left(\sqrt{n(t)} - \sqrt{n^*}\right) \\ &\quad + \tfrac{2\sqrt{N}}{\beta h^{3/2}}\left(\tanh^{-1}\sqrt{\tfrac{hn(t)}{N}} - \tanh^{-1}\sqrt{\tfrac{hn^*}{N}}\right) && \text{if } t > t^* \end{aligned} \quad [2]$$

where the inflection point is given by $t^* = \frac{2}{\beta}\left(\sqrt{\frac{N}{h+1}} - \sqrt{n_0}\right)$ and $n^* = \frac{N}{h+1}$. The solution, shown by the solid lines in Fig. 3*E*, exhibits close agreement to the expansion rates observed for ant rafts up to $N = 7{,}000$ ants.

Modifications to this model are possible to increase its accuracy. For example, ants at the bottom will at times exchange positions with those on top. However, these rates are slow and, during construction, such negative feedback is not required because the rate of raft expansion is controlled by the number of ants remaining on top. We also implemented a Brownian diffusion model (34) (see *SI Text*), but found that it was unable to account for the high rate of growth of the raft.

Discussion

Overlooking its diminutive size and shortcomings in soapy solutions, the ant raft has attractive traits with respect to man-made flotation devices. It simultaneously provides cohesion, buoyancy, and water repellency to its passengers. It can be constructed quickly (in approximately 100 s) without any additional equipment. It can accommodate thousands to millions of passengers with zero casualties. But perhaps most strikingly, the ant raft is self-assembling.

Many of these benefits are due to the ant's small size. At the scale of millimeters, ants have great strength, high speed, and the ability to trap air pockets when submerged, which in turn makes their rafts water repellent. These abilities will likely vanish at large sizes. Roboticists interested in building biomimetic ant rafts will need to design robots that can both reversibly attach to and traverse over one another. Moreover, they will need to understand which processes of raft assembly process are coordinated (such as ant-to-ant gripping) as opposed to stochastic (ant trajectories).

In the ant raft, passengers are used interchangeably as flotation devices. This feature of the raft makes its construction reversible. We conducted experiments in which free ants were moved one-by-one from the top of the raft. This removal caused the raft to self-heal: Ants on the bottom moved to the top to preserve the average raft thickness. We surmise that ants are able to sense how many of their colony members are walking on top of them. Similar behavior was shown to be important in ant bridge construction in which bridges of ants were maintained as long as ants were crossing the bridges (9).

Self-assembly and self-healing are hallmarks of living organisms (35, 36). The ant raft demonstrates both these abilities, providing another example that an ant colony behaves like a superorganism (7). In addition, we observed that large numbers of organisms can behave similarly to a fluid. This viewpoint has been used to model the flow in human crowds (37). Understanding ant rafts also requires an additional consideration—namely, that they are water repellent en masse. Future studies of swarms of other insects may find they too exhibit an aversion or repellency to water or rain that affects their cooperative behaviors.

Methods

Time-Lapse Video. Ants were scooped with spoons into 100-mL beakers rimmed with talc powder and weighed to count their numbers. Using the natural adhesion of the ants, a few swirls of the beaker was sufficient to roll the ants into balls (Fig. 3*C*). Ant balls were placed on the water surface and held stationary by impalement upon a pair of wires of an inverted light-emitting diode affixed to the aquarium bottom. Top and side views of the ant raft were filmed using a high-definition digital video camera (Sony HDR-HC9). Fluid distortion of the side view of the raft was minimized by filming through a glass sheet coated with Fluoropel™. Films were digitized using Matlab to determine the area of the raft as a function of time.

Cohesive Force. We glued a live ant onto the bottom of a glass slide. Clinging to this ant was another ant, harnessed with an elastic band (length 5 cm, diameter 1 mm). By pulling on the elastic slowly (for a duration of 3 s),

the maximum extension (5–7 mm) of the band was measured upon release of the ant's grip. In the measurements reported, we subtracted the 1-mm extension of the ant's arms. Tensile force was estimated using the spring constant of the elastic (0.20 N/m).

Ant Viscosity. To measure viscosity, we measured the settling speed $U \sim 10^{-2}$ cm/s of a sphere of radius $a = 4.8$ mm and density $\rho_s = 7.5$ g/mL in an ant raft of 8,000 ants floating in a water-filled beaker of radius $3a$. Settling speed was estimated using the height of the raft and the duration elapsed before the sphere exited the raft. Stokes drag on this system indicates that the viscosity $\mu = \frac{2}{9}(\rho_s - \rho)ga^2/U$.

Ant Separation Distance. To measure the distance between ant centers-of-mass, rafts of ants were frozen in liquid nitrogen. Ants were removed manually until a single layer remained, whose number of ants was counted manually.

Bounce probability. We measured the bounce probability by tracking the motion of ants constructing their raft. Specifically, we observed a raft of 500 ants for 20 s, tracking five separate points on the raft's circumference. During this duration, we could distinguish the motion of 9–16 ants at each point. In terms of X, the number of ants ricocheting, and Y, the number adhering, the bounce probability was found to be $p = X/(X + Y) = 0.64 \pm 0.04$ ($N = 5$).

ACKNOWLEDGMENTS. The authors thank S. Bair and P. Neitzel for useful discussions, V. Breedveld, M. Goodisman, and S. Shinotsuka for laboratory assistance, and the National Science Foundation for support (IOS-0920402).

1. Sumpter D (2006) The principles of collective animal behaviour. *Philos Trans R Soc Lond B Biol Sci* 361:5–22.
2. Couzin ID, Krause J (2003) Self-organization and collective behavior in vertebrates. *Adv Study Behav* 32:1–75.
3. Parrish JK, Edelstein-Keshet L (1999) Complexity, patterns, and evolutionary trade-offs in animal aggregation. *Science* 284:99–101.
4. Garnier S, Gautrais J, Theraulaz G (2007) The biological principles of swarm intelligence. *Swarm Intell* 1:3–31.
5. Yim M, et al. (2007) Modular self-reconfigurable robot systems [grand challenges of robotics]. *IEEE Robot Autom Mag* 14:43–52.
6. Brooks R, Flynn A (1989) Fast, cheap, and out of control: A robot invasion of the solar system. *J Br Interplanet Soc* 42:478–485.
7. Hölldobler B, Wilson E (1990) *The Ants* (Belknap, Cambridge, MA).
8. Tschinkel W (2006) *The Fire Ants* (Belknap, Cambridge, MA) p 25.
9. Anderson C, Theraulaz G, Deneubourg JL (2002) Self-assemblages in insect societies. *Insectes Soc* 49:99–110.
10. Bonabeau E, et al. (1998) Dripping faucet with ants. *Phys Rev E Stat Nonlin Soft Matter Phys* 57:5904–5907.
11. Schneirla T, Topoff H (1971) *Army Ants: A Study in Social Organization* (Freeman, San Francisco) p 56.
12. Haight KL (2006) Defensiveness of the fire ant *solenopsis invicta*, is increased during colony rafting. *Insectes Soc* 53:32–36.
13. McGrail S (2008) *Ancient Boats and Ships* (Shire Publ, Buckinhamshire, UK) p 29.
14. Highsmith R (1985) *Floating and algal rafting as potential dispersal mechanisms in brooding invertebrates*, , Marine Ecology Progress Series (Oldendorf, Luhe, Germany), 25, pp 169–179.
15. Bush JWM, Hu DL (2006) Walking on water: Biolocomotion at the interface. *Annu Rev Fluid Mech* 38:339–369.
16. Hu DL, Prakash M, Chan B, Bush JWM (2007) Water-walking devices. *Exp Fluids* 43:769–778.
17. Suhr SH, Song YS, Lee SJ, Sitti M (2005) Biologically inspired miniature water strider robot. *Robot Sci Syst I* 319–325.
18. Federle W, Riehle M, Curtis ASG, Full RJ (2002) An integrative study of insect adhesion: Mechanics and wet adhesion of pretarsal pads in ants. *Integr Comp Biol* 42:1100–1106.
19. Dejean A, et al. (2010) Arboreal ants use the Velcro® Principle to capture very large prey. *PloS One* 5:e11331.
20. Federle W, Rohrseitz K, Holldobler B (2000) Attachment forces of ants measured with a centrifuge: Better "wax-runners" have a poorer attachment to a smooth surface. *J Exp Biol* 203:505–512.
21. Federle W, Endlein T (2004) Locomotion and adhesion: Dynamic control of adhesive surface contact in ants. *Arthropod Struct Dev* 33:67–75.
22. Gorb S (2001) *Attachment Devices of Insect Cuticle* (Kluwer, Dordrecht, The Netherlands), pp 164–165.
23. Cassill D, Greco A, Silwal R, Wang X (2007) Opposable spines facilitate fine and gross object manipulation in fire ants. *Naturwissenschaften* 94:326–332.
24. Stewart H (2006) Ontogenetic changes in buoyancy, breaking strength, extensibility, and reproductive investment in a drifting macroalga *Turbinaria ornata* (Phaeophyta). *J Phycol* 42:43–50.
25. Hu DL, Bush JWM (2005) Meniscus-climbing insects. *Nature* 437:733–736.
26. Neinhuis C, Barthlott W (1997) Characterization and distribution of water-repellent, self-cleaning plant surfaces. *Ann Bot* 79:667–677.
27. Gao X, Jiang L (2004) Water-repellent legs of water striders. *Nature* 432:36.
28. Bush J, Hu D, Prakash M (2007) The integument of water-walking arthropods: Form and function. *Adv in Insect Phys* 34:117–192.
29. De Gennes P, Brochard-Wyart F, Quere D (2004) *Capillarity and Wetting Phenomena: Drops, Bubbles, Pearls, Waves* (Springer, New York).
30. Quéré D (2008) Wetting and roughness. *Annu Rev Mater Res* 38:71–99.
31. Yarin A (2006) Drop impact dynamics: Splashing, spreading, receding, bouncing. *Annual Rev Fluid Mech* 38:159–192.
32. Rafai S, Bonn D, Boudaoud A (2004) Spreading of non-Newtonian fluids on hydrophilic surfaces. *J Fluid Mech* 513:77–85.
33. Brochard-Wyart F, Debr'egeas G, Gennes P (1996) Spreading of viscous droplets on a non viscous liquid. *Colloid Polym Sci* 274:70–72.
34. Øksendal B (2003) *Stochastic Differential Equations: An Introduction with Applications* (Springer , New York) p 125.
35. Whitesides G, Grzybowski B (2002) Self-assembly at all scales. *Science* 295:2418–2421.
36. Wool RP (2008) Self-healing materials: A review. *Soft Matter* 4:400–418.
37. Hughes R (2003) The flow of human crowds. *Annu Rev Fluid Mech* 35:169–182.

Supporting Information

Mlot et al. 10.1073/pnas.1016658108

SI Text

Experiments of Ant Rafts in Soap Solutions. We find that even trace amounts will cause the ants to radically change their behavior, as shown in the images of a raft on water with traces of soap (Fig. S1). As soon as ants become even slightly soapy, they immediately release their grip with each other, which is shown by the disintegration of the raft and its submergence underwater. This is in contrast to the closely packed ants in the buoyant raft, as shown in Figs. 1 and 2 in the main text.

Differential Equation Models of Ant-Raft Formation. ***Straight movement in random direction model.*** Let N equal the total number of ants. Let t denote time in seconds. Let $n(t)$ denote the number of ants in the bottom layer at time t equal to the area of the raft at time t. The number of ants in the bottom layer can be converted to square centimeters with conversion factor 34 ants = 1 cm^2. Let h denote the eventual thickness of the raft, experimentally determined to be approximately 2.5 (ant heights). In the straight movement model, we assume that only ants in the top layer move, and they move by picking a random direction and going straight until they hit a boundary. When they hit a boundary, they "bounce" with probability $p = 0.65$ (this value determined by observation), picking a random direction away from the boundary, and "stick" with probability $1-p$. If they bounce, they go again until they hit a boundary, where again they bounce with probability p and stick with probability $1-p$. They repeat this process until they stick, at which time they join the bottom h layers there. The expected number of "bounces" before sticking is therefore $\frac{1}{1-p} - 1 = 1.86$.

Lemma 1. *Let x be a random point in a circle of radius r, and let θ be a direction randomly chosen from the interval $[0,2\pi]$. Then the expected distance from x to the circle boundary, in the direction θ, equals $\frac{8r}{3\pi} \approx 0.8488r$. Now let x be a point on the circle boundary and let θ be a direction randomly chosen from the interval $[0,\pi]$ where $\theta = \pi/2$ means the direction toward the circle center. Then the expected distance from x to the circle boundary in the direction θ equals $4r/\pi \approx 1.27r$.*

The Proof is given in *Calculus derivations* so as not to disrupt the exposition of the model.

Let u denote the speed of an ant in centimeters per second. When $N \geq (h+1)n(t)$, there is a full top layer of ants who can move. A single ant in that layer takes on average $[0.849+(1.86)(1.27)]r/u = 3.21r/u$ s to reach a boundary and stick, where $\pi r^2 = n(t)/34$ so $r = \sqrt{n(t)/34\pi}$ is the radius of the raft in centimeters. There are $n(t)$ ants in the moving layer so, on average, $n(t)u/3.21r$ ants reach and stick to the boundary per second, equaling $\sqrt{34\pi n(t)}u/3.21$ ants per second. These ants form a new exterior boundary h ants thick. So,

$$\frac{dn(t)}{dt} = u\sqrt{34\pi n(t)}/3.21 \text{ h}.$$

When $hn(t) \leq N \leq (h+1)n(t)$, there is a partial layer of $N - hn(t)$ ants who can move. So,

$$\begin{aligned}\frac{dn(t)}{dt} &= u[N - hn(t)]/3.21 \text{ hr} \\ &= u\sqrt{34\pi}[N - hn(t)]/3.21 \text{ h}\sqrt{n(t)}.\end{aligned}$$

Brownian motion model. Let N,t,$n(t)$,h be as in the Straight Motion Model. We assume that only ants in the top layer move, and they move in Brownian motion until they hit a boundary. It is more or less obvious that the expected time to reach a boundary from the center of a circle of radius r is r^2 (up to scaling by ant speed). It is not as obvious what the expected time to reach a boundary is from a random point in the circle.

Lemma 2. *Let x be a random point in a circle of radius r. Execute standard Brownian motion from x. The expected time until the circle boundary is reached is $r^2/4$.*

Proof: From Øksendal (1), the expected first hitting time is $(r^2 - |x|^2)/2$ where $|x|^2$ is the squared distance to the circle center from x. The rest is calculus, given later.

When $N \geq (h+1)n(t)$, there is a full top layer of ants who can move. A single ant in that layer takes $r^2/4 = n(t)/136\pi$ s to reach a boundary, because $\pi r^2 = n(t)/34$. There are $n(t)$ ants in the moving layer so, on average, $136\pi n(t)/n(t) = 136\pi$ ants reach the boundary per second. Notice this number is independent of the size of the raft and of N:

$$\frac{dn(t)}{dt} = 136\pi/h.$$

When $hn(t) \leq N \leq (h+1)n(t)$, we have $N - hn(t)$ ants in the moving layer. On average, $136\pi[N - hn(t)]/n(t)$ reach the boundary per second. For this time period,

$$\frac{dn(t)}{dt} = 136\pi[N - hn(t)]/hn(t).$$

Note, this model has to be scaled by some unknown factor, which is the ant speed, but the ant speed here is not the usual centimeters per second, but rather the Brownian motion scaling compared with standard Brownian motion. This model's predictions do not match the data. In the data, rafts grow faster when N is bigger. We changed the model to let every ant except those in the lowest h layers move. The formula is simply the second formula used for all t, that is,

$$\frac{dn(t)}{dt} = 136\pi[N - hn(t)]/hn(t).$$

However, this model did not fit the data, either.

Calculus derivations. For the Brownian Motion Model, we want the average value of $(r^2 - x^2)/2$ in a circle of radius r, where x^2 is the squared distance to the circle center, which is

$$\frac{1}{\pi r^2}\int_{x=0}^{r} \frac{r^2 - x^2}{2} 2\pi x dx = r^2/4.$$

For the Straight Motion Model, we first need a geometric lemma. Suppose the ant is at distance x from the circle center. Consider the chord that is perpendicular to the line segment from the circle center to the ant and passes through the ant. Let z denote the length of the chord. Then $(z/2)^2 = (r-x)(r+x)$ whence $z/2 = \sqrt{r^2 - x^2}$. Now suppose the ant moves at angle θ

to the chord. If $\theta = 0$ or $\theta = \pi$, the distance to the circle boundary is $z/2$. If $\theta = \pi/2$, the distance is $r + x$ and if $\theta = 3\pi/2$ the distance is $r - x$. We need a formula for the general case of θ. By symmetry, it suffices to consider the cases $0 \leq \theta \leq \pi/2$; $\pi \leq \theta \leq 3\pi/2$. The two cases θ, $\theta + \pi$ define a chord passing through the ant. Let y denote the length of the shorter segment of the chord (where the chord intersects the ant). Then the longer segment has length $2x \sin\theta + y$, from which we obtain

$$y(2x\sin\theta + y) = (r - x)(r + x) \Rightarrow y^2 + 2x\sin\theta y - (r^2 - x^2) = 0.$$

One of the roots to this quadratic is negative. Hence,

$$y = -x\sin\theta + \sqrt{x^2\sin^2\theta + (r^2 - x^2)}.$$

If the ant randomly chooses between θ and $\theta + \pi$, the expected distance traveled is $\frac{1}{2}(2x\sin\theta + 2y) = \sqrt{x^2\sin^2\theta + r^2 - x^2} = \sqrt{r^2 - x^2\cos^2\theta}$. (Check this formulation against the two extremes: When $\theta = \pi/2$, we have $\cos\theta = 0$ and the expected distance is r, which is correct. When $\theta = 0$, we have $\cos\theta = 1$ and the expected distance is $\sqrt{r^2 - x^2} = z/2$, which is correct.)

We assume that the ant chooses a random direction. The expected distance traveled by the ant to a boundary is therefore

$$\frac{2}{\pi}\int_0^{\pi/2} \sqrt{r^2 - x^2\cos^2\theta}\,d\theta.$$

Taking the mean value of this individual expected distance as x ranges from 0 to r gives an overall expected distance of

$$\frac{1}{\pi r^2}\int_0^r 2\pi x dx \int_0^{\pi/2} \frac{2}{\pi}\sqrt{r^2 - x^2\cos^2\theta}\,d\theta.$$

Putting the factor of r on the left (which is obvious by scaling; we could have done it earlier) gives

$$r\int_0^1 4x/\pi dx \int_0^{\pi/2} \sqrt{1 - x^2\cos^2\theta}\,d\theta = 8r/3\pi \approx 0.8488r.$$

The integral was calculated both numerically and with Mathematica 7. (Check this integral against the two extremes. At the two extremes of integration, the values are $2r/\pi$ at $x = r$, and r at $x = 0$. The average value ought to be somewhere between $0.64 \approx 2/\pi$ and 1.)

After the ant reaches the boundary, the situation is slightly different. We assume that the ant moves in a random direction *away* from the boundary. In terms of our model, we assume that the ant chooses a random value of θ from the interval $0 \leq \theta \leq \pi$. The expected distance to the (next) boundary is

$$\frac{2}{\pi}r\int_0^{\pi/2} 2\sqrt{1 - \cos^2\theta}\,d\theta = \frac{4r}{\pi}\int_0^{\pi/2} \sin\theta d\theta = \frac{4r}{\pi} = 1.27r.$$

1. Øksendal B, (2003) *Stochastic Differential Equations: An Introduction with Applications* (New York, Springer), 6th Ed, p 125.

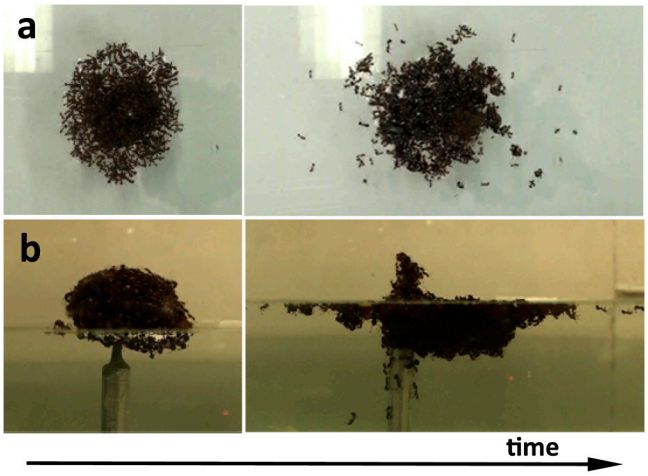

Fig. S1. Raft of 3,000 ants exposed to traces of surfactant: (*A*) top view; (*B*) side view.

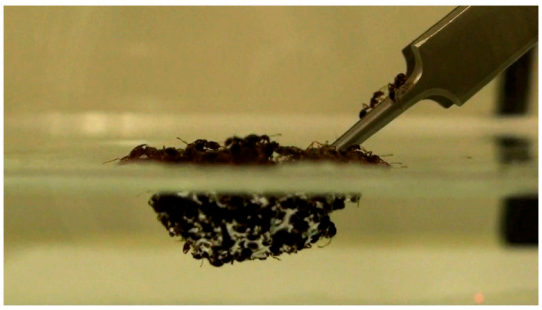

Movie S1. A raft of 500 ants pushed underwater using tweezers. The glistening sheen marks the presence of an air-layer waterproofing the raft.
Movie S1 (MOV)

Movie S2. Panoramic view of an ant raft, showing the ant–water contact line. Time sped up 2×.
Movie S2 (MOV)

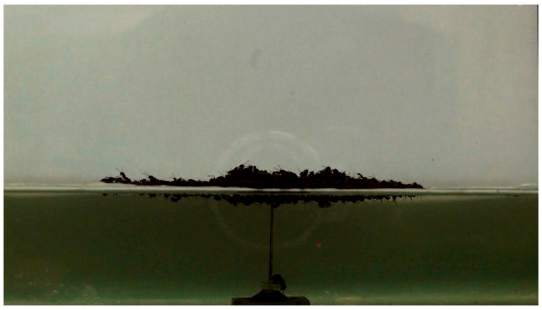

Movie S3. Side view of 3,000 ants constructing a raft. The green fluid is water, atop which is air. At all times during the raft construction, the top layer of ants remain dry, floating atop a wetted bottom layer of ants. Time sped up 8×.
Movie S3 (MOV)

Movie S4. Top view of 3,000 ants constructing a raft. A sphere of ants is placed on the water surface. Upon contact with water, ants from the center of the raft scramble radially outward, adding to the raft's edge until generating an equilibrium shape of the raft resembling a pancake. Time sped up 8×.

Movie S4 (MOV)

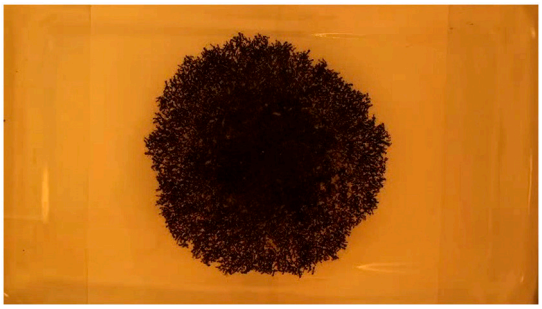

Movie S5. Top view of 8,000 ants constructing a raft. Although this raft was the largest we studied, rafts of hundreds of thousands of fire ants can be observed in the wild. Time sped up 15×.

Movie S5 (MOV)